Discriminating dynamic regimes using measures of causality networks from multivariate time series

Christos Koutlis and Dimitris Kugiumtzis

[1]Department of Electrical and Computer Engineering,
Aristotle University of Thessaloniki, Greece,
Email: ckoutlis@auth.gr, dkugiu@auth.gr

Abstract—In many applications ranging from neurophysiology to finance, the dynamics of the underlying mechanism to observed multivariate time series is believed to change and this is reflected to the inter-dependence structure of the observed variables. We consider a Granger causality index for estimating the inter-dependence structure and form causality networks with nodes the observed variables and directed connections given by the selected Granger causality index. The focus of the study is on assessing the different network measures as to their ability in discriminating different dynamic regimes of the system underlying the multivariate time series. For this, we first compute the network measures on many realizations of the coupled Mackey-Glass system under different coupling structures, and then to electroencephalogram recordings containing episodes of epileptiform discharges. The ranking of the network measures on the simulated and real data revealed the same subset of measures performing best.

1. Introduction

The investigation of complex networks with directed connections derived by Granger causality indices between the variables of multivariate time series being the network nodes has gained interest in many research fields such as finance and electroencephalogram (EEG) analysis [1, 2]. In complex network analysis a number of measures have been proposed to extract information about the network structure, and subsequently the underlying mechanism of the observed time series. The ability of network measures to discriminate different dynamic regimes has been a topic of research, e.g. in brain connectivity [3, 4].

In this work, we pursue a simulation study and rank network measures in terms of their ability to discriminate different network structures in causality networks of time series produced by the coupled Mackey Glass system. Further, we apply the same setup to EEG data in an attempt to identify changes in the brain connectivity structure before, during and after epileptiform discharges terminated by transcranial magnetic stimulation (TMS). As a Granger causality index we use the measure of partial mutual information from mixed embedding (PMIME) [5].

The structure of the paper is as follows. In Section 2, the data sets, the Granger causality index PMIME and the network measures are briefly described. In Section 3, the results of the simulations and the EEG analysis are presented and discussed, and in Section 4 conclusions are given.

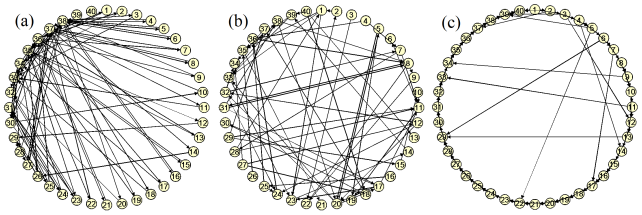

Figure 1: Network structures: (a) Scale-free, (b) Random, (c) Small world

2. Material and methods

2.1. Simulated and EEG data

For the simulation study, we consider the coupled Mackey-Glass system. The Mackey-Glass system is a chaotic system given by a delay differential equation of one variable [6], and it has been extended to coupled variables [7, 5]. Here, for the first time it is used for as many as 40 variables given as

$$\dot{x}_i(t) = -0.1x_i(t) + \sum_{j=1}^{40} \frac{c_{ij}x_j(t-\Delta)}{1+x_j(t-\Delta)^{10}}, \quad i = 1,2,\ldots,40, \tag{1}$$

where c_{ij} is the directed coupling strength reading from $x_j(t)$ to $x_i(t)$ when $i \neq j$ and $c_{ii} = 0.2$. Our interest is in high-dimensional dynamics and thus we set $\Delta = 100$, which for the univariate case corresponds to a fractal dimension of about 7 [8]. The coupling strength matrix $C = \{c_{ij}\}$ arises from any of the three network types: (a) a scale-free network obtained by the method of preferential attachment, (b) a random network of the Erdös-Rényi model, and (c) a small world network, as shown in Fig. 1. For the generated adjacency matrix of each network, we assign a weight matrix $C = \{c_{ij}\}$ of the same coupling strength and we consider a weak coupling strength of 0.1 and a strong coupling strength of 0.5 at the level of generalized synchronization, as assessed by the method of the auxiliary system [9]. To obtain statistically valid results we generate 100 time se-

ries from the coupled Mackey-Glass system with coupling structure given by each of the three network types.

The EEG analysis is done on two EEG recordings of two epileptic patients. The patients exhibited interictal discharges and subclinical epileptic seizures, collectively termed epileptiform discharges (ED), which turned out to be terminated by the administration of a block of 5 transcranial magnetic stimulations (TMS). In total, there are 25 episodes of EDs terminated by TMS, 13 for the first and 12 for the second recording. The EEG was processed so that TMS artifact was replaced [10], and the data were re-referenced to infinity, bandpass filtered to $[0.01, 70]Hz$ and down-sampled from 1450 Hz to 200 Hz. After rejection of bad channels there were 45 channels for the first recording and 34 channels for the second recording. Each episode comprises 10 s before the ED, the ED, and 10 s after the ED. The Granger causality index of PMIME is computed on sliding windows of 2 s with a sliding step of 0.5 s. Here, three network structures are considered, before the ED, during the ED, and after the ED.

2.2. The Granger causality index

We attempt to form a causality network from each multivariate time series described in Sec. 2.1. Each directed connection in the causality network is defined by the Granger causality index from the driving variable towards the response variable.

As Granger causality index, we use the recently proposed measure of partial mutual information from mixed embedding (PMIME) [5] because it is a direct causality measure that can deal with a large number of variables. The PMIME is based on the mutual information (MI) and the conditional MI (CMI), and for their estimation the k-nearest neighbors estimate is used. The basic idea of the PMIME is the following. Say we observe K time series and we want to quantify the causality effect (or information flow) from X to Y given the rest $K-2$ variables denoted as Z. First, we construct a mixed embedding vector $\mathbf{w}_t$ of the most relevant delays from all K variables that explains best the evolution of Y, y_{t+1}, according to a criterion of redundancy and relevance facilitated by CMI. The presence of lagged components of X, $\mathbf{w}_t^x$ in $\mathbf{w}_t$ indicates that X has some effect on the evolution of Y (and the same for Y and Z), and this is quantified by the CMI $I(y_{t+1};\mathbf{w}_t^x\,|\,\mathbf{w}^y,\mathbf{w}^z)$. The PMIME is obtained by normalizing this CMI by the total MI, $R_{X\to Y|Z} = I(y_{t+1};\mathbf{w}_t^x\,|\,\mathbf{w}^y,\mathbf{w}^z)/I(y_{t+1};\mathbf{w}_t)$. If there is causal effect from X to Y the PMIME is positive, whereas the absence of lagged components of X indicates no causal effect and then the PMIME is exactly zero. Thus a unweighted network is derived in a straightforward way by setting any positive PMIME value to one.

2.3. Network measures

A number of network measures listed in Table 1, believed to capture different characteristics of the network structure [4], are computed on causality networks derived from time series of simulated and EEG data. The average

Symbol	Description
$\bar{C}$	Average clustering coefficient
$\bar{g}$	Average betweenness centrality
l_G	Characteristic path length; the average shortest path length in the network
GE	Global efficiency; the average inverse shortest path length in the network
$\bar{\epsilon}$	Average eccentricity
d	Diameter
$\overline{deg}$	Average degree
$\overline{str}$	Average strength
r_{deg}	Assortativity coefficient in terms of the degree
r_{str}	Assortativity coefficient in terms of the strength
kcs	k-core size, k=3
ϕ	Rich club coefficient, k=3

Table 1: List of network measures

clustering coefficient ($\bar{C}$) is used as a measure of functional segregation and the characteristic path length (l_G) as well as the global efficiency (GE), the average eccentricity ($\bar{\epsilon}$) and the diameter (d) are used as measures of functional integration. We also use as measures of centrality the average betweenness centrality ($\bar{g}$), the average degree ($\overline{deg}$) and the average strength ($\overline{str}$). As a measure of resilience we compute the assortativity coefficient (r_{deg} and r_{str}), i.e. a correlation coefficient between the degrees or strengths of all nodes on two opposite ends of a link for in-in, in-out, out-in and out-out degrees and strengths of the nodes and for the undirected graph as well. Finally, we compute as measures of the core structure the k-core size, i.e. the number of nodes with degree k or higher for $k=3$ and the rich club coefficient, i.e. the density of the k-core for $k=3$ [4].

We compute all these network measures in order to assess the network characteristics quantified by the measures that best classify the time series to the correct network type for the simulated data, and the pre-ED vs ED, and post-ED vs ED for the EEG data.

2.4. Evaluation of the measures

In order to distinguish the network measures presented in Sec. 2.3 having the ability to discriminate certain dynamic regimes, we applied the non-parametric Wilcoxon rank-sum test for independent samples to rank the measures according to their p-value. Moreover, we used the index of the area under receiver operating characteristic curve (AUROC) for each pair of different dynamic regimes [11], e.g. time series generated by a coupling strength of scale-free network vs random network.

For both simulated and real data, we computed a score

for each network measure i and for each comparison of dynamic regimes on the basis of the Wilcoxon test

$$S_i = \begin{cases} 1 - \frac{1-r_i}{D} & \text{if } p_i \leq 0.05 \\ 0 & \text{if } p_i > 0.05 \end{cases} \quad (2)$$

where p_i is the p-value of the test with the i-measure and r_i denotes the ranking of the i-measure among the D measures that reached a p-value less or equal than 0.05. The score is designed to take values from 0 to 1, where 1 is the best score value meaning that the i-measure obtained the smallest p-value, and 0 corresponds to no discrimination ($p_i > 0.05$). To assess the overall performance of each measure in all discriminating tasks, we obtain the average score $\bar{S}_i$ over all comparisons of dynamic regimes. For the real data, first the average score is obtained from each episode for each network measure over the windows of 2 s at each comparison (pre-ED vs ED, and ED vs post-ED), and then a grand average is obtained over all episodes.

3. Results

3.1. Simulated data

We obtain six ranking scores for each measure, for the comparisons of the three coupling network types (Scale-free vs. Random, Scale-free vs. Small world, Random vs. Small world) and the two coupling strengths (0.1 and 0.5). The ranking lists of the network measures that reached AUROC > 0.65 are given in Table 2 (results are not shown for Random vs. Small world and coupling strength 0.1 as none of the measures obtained AUROC > 0.65). The best results were achieved in the discrimination of Scale free vs. Small world and high coupling strength. Also some measures as $\overline{str}$, $\overline{deg}$ and $\bar{C}$ score highest in most discrimination tasks.

In Table 3, the top 10 network measures with respect to the average score are listed together with their average AUROC value. A first observation is that the average strength scores highest while the average degree is left much behind indicating the advantage of having weighted rather than unweighted networks, i.e. using the value of the Granger causality index rather than its significance. The second best measure of the rich club coefficient is essentially the same as the average strength as in most cases the k-core is the whole network. The third highest scoring measure of the characteristic path length captures indeed a different characteristic of network structure that may be complementary to the average strength. However, the average AUROC of all network measures is not very high and this is partly due to the inability of PMIME to capture the initial coupling structure, but also to the difficulty of the discriminating task involving high-dimensional and complex dynamics.

3.2. EEG data

An example of the profile of four network measures from one ED episode are shown in Fig. 2. The average degree quantifies a decrease of brain connectivity during ED (fewer connections), whereas the global clustering coefficient detects this change at a lesser degree, whereas the other two measures do not seem to change systematically throughout the episode.

Measure	AUROC	Measure	AUROC
Scale free-Random Coupling strength 0.1		Scale free-Random Coupling strength 0.5	
$\overline{str}$	0.813	$\overline{str}$	0.794
ϕ	0.721	$\overline{deg}$	0.776
l_G	0.712	$\bar{C}$	0.732
kcs	0.683	d	0.725
$\bar{\epsilon}$	0.680	$r_{deg}(out, in)$	0.670
$\overline{deg}$	0.679	$r_{deg}(out, out)$	0.668
$\bar{C}$	0.656	GE	0.656
Scale free-Small world Coupling strength 0.1		$r_{str}(out, in)$	0.654
$\overline{str}$	0.796	Scale free-Small world Coupling strength 0.5	
$\bar{C}$	0.752	$\bar{C}$	0.877
ϕ	0.746	$\overline{deg}$	0.793
$r_{str}(out, in)$	0.710	d	0.770
Random-Small world Coupling strength 0.5		kcs	0.746
kcs	0.763	$\overline{str}$	0.739
$r_{deg}(out, in)$	0.740	GE	0.700
$r_{str}(in, in)$	0.721	$r_{str}(in, out)$	0.685
$\overline{str}$	0.688	$r_{deg}(in, in)$	0.658

Table 2: Ranking of the network measures according to their score.

The same setup for evaluation of network measures was applied to the EEG data and the total results similar to these in Table 3 are given in Table 4. Here, both average strength and average degree are highest with average eccentricity scoring also highest. The discrimination of ED from pre-ED and post-ED is successfully detected with many network measures as their average AUROC is very high, indicating the drastic change of brain connectivity structure with the ED.

4. Conclusions

Some network measures exhibited good performance in discriminating different network structures derived from multivariate time series. Also the top seven ranked measures are the same in the simulation and the real data analysis, indicating the usefulness of these measures. Finally, the PMIME performed well detecting the network type in the simulation study but could not detect all the true connections. We plan to investigate further the performance of PMIME compared to other Granger causality measures and include other simulated systems that exhibit EEG-like oscillations.

Measure	Score	mean AUROC
$\overline{str}$	1.00	0.74
ϕ	0.91	0.62
l_G	0.81	0.63
$\bar{\epsilon}$	0.72	0.57
$\bar{C}$	0.62	0.71
$\overline{deg}$	0.52	0.67
d	0.43	0.64
GE	0.33	0.62
$r_{str}(out, in)$	0.24	0.63
kcs	0.17	0.66

Table 3: Average score and average AUROC value of the network measures for the simulated data.

Measure	Score	mean AUROC
$\overline{deg}$	0.62	0.97
$\bar{\epsilon}$	0.60	0.94
$\overline{str}$	0.50	0.97
$\bar{C}$	0.41	0.90
ϕ	0.38	0.96
d	0.38	0.90
l_G	0.32	0.86
$\bar{g}$	0.23	0.79
GE	0.12	0.74
$r_{str}(undirected)$	0.07	0.70

Table 4: Average score and average AUROC value of the network measures for the EEG data.

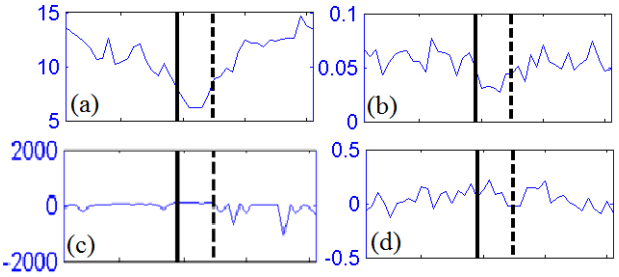

Figure 2: The network measure performance before the ED, during the ED (after the solid line and before the dashed line) and after the ED of one episode. (a) Average degree, (b) global clustering coefficient, (c) characteristic path length, (d) assortativity coefficient for undirected graph.

Acknowledgement

The authors would like to thank Vasilios K. Kimiskidis, Professor of Neurology at Aristotle University of Thessaloniki, for making available the EEG data. The work is supported by the Greek General Secretariat for Research and Technology (Aristeia II, No 4822).

References

[1] Monica Billio, Mila Getmansky, Andrew W. Lo, and Loriana Pelizzon. Econometric measures of connectedness and systemic risk in the finance and insurance sectors. *Journal of Financial Economics*, 104(3):535 – 559, 2012. Market Institutions, Financial Market Risks and Financial Crisis.

[2] Ali Khadem and Gholam-Ali Hossein-Zadeh. Estimation of direct nonlinear effective connectivity using information theory and multilayer perceptron. *Journal of Neuroscience Methods*, 229(0):53 – 67, 2014.

[3] Danielle S. Bassett, Edward Bullmore, Beth A. Verchinski, Venkata S. Mattay, Daniel R. Weinberger, and Andreas Meyer-Lindenberg. Hierarchical organization of human cortical networks in health and schizophrenia. *The Journal of Neuroscience*, 28(37):9239–9248, 2008.

[4] M. Rubinov and O. Sporns. Complex network measures of brain connectivity: Uses and interpretations. *NEUROIMAGE*, 52(3):1059–1069, 2010.

[5] D. Kugiumtzis. Direct-coupling information measure from nonuniform embedding. *Physical Review E*, 87:062918, 2013.

[6] M. Mackey and L. Glass. Oscillation and chaos in physiological control systems. *Science*, 197:287, 1977.

[7] D. V. Senthilkumar, M. Lakshmanan, and J. Kurths. Transition from phase to generalized synchronization in time-delay systems. *Chaos: An Interdisciplinary Journal of Nonlinear Science*, 18(2):023118, 2008.

[8] M. Ding, C. Grebogi, E. Ott, T. Sauer, and J. A. Yorke. Estimating correlation dimension from a chaotic time series: when does a plateau onset occur? *Physica D*, 69:404–424, 1993.

[9] S. Acharyya and R.E. Amritkar. Generalized synchronization of coupled chaotic systems. *The European Physical Journal Special Topics*, 222(3-4):939–952, 2013.

[10] V. K. Kimiskidis, D. Kugiumtzis, S. Papagiannopoulos, and N. Vlaikidis. Transcranial magnetic stimulation (TMS) modulates epileptiform discharges in patients with frontal lobe epilepsy: a preliminary EEG-TMS study. *International Journal of Neural Systems*, 23(01):1250035, 2013.

[11] T. Fawcett. An introduction to roc analysis. *Pattern Recognition Letters*, 27(8):861–874, 2006. cited By (since 1996)2503.